Tracking of particles in froth using neutron imaging

Heitkam, S.; Lappan, T.; Eckert, S.; Trtik, P.; Eckert, K.;

Originally published:

April 2019

Chemie Ingenieur Technik 91(2019)7, 1001-1007

DOI: https://doi.org/10.1002/cite.201800127

Perma-Link to Publication Repository of HZDR:

https://www.hzdr.de/publications/Publ-28156

Tracking of particles in froth using neutron imaging

S. Heitkam[1,2], T. Lappan[1], S. Eckert[1], P. Trtik[3], K. Eckert[1,2]

[1] Helmholtz-Zentrum Dresden-Rossendorf, Institute of Fluid Dynamics, 01328 Dresden, Germany
[2] Technische Universität Dresden, Institute of Process Engineering and Environmental Technology, 01062 Dresden, Germany
[3] Paul Scherrer Institut, Laboratory for Neutron Scattering and Imaging, 5232 Villigen PSI, Switzerland

Keywords: Froth, Particle laden Foam, Particle Tracking, Neutron Radiography, Neutron Imaging

Abstract

In this study, neutron imaging is employed to investigate the movement of hydrophobic particles in a rising froth column. A cylindrical batch-flotation cell is mounted to a rotary stage, allowing for three-dimensional analysis. Gadolinium particles of 200 µm diameter are hydrophobized and floated by means of small air bubbles. The generated froth is investigated by neutron imaging. Using particle-tracking and a reconstruction algorithm for the third dimension, the movement of particles in the froth is analyzed. Varying the concentration of the frother sodium oleate, different froth stabilities are compared. It has been found, that with decreasing froth stability bubble rupture leads to higher horizontal diffusion of particles and to higher agglomeration of particles.

1 Introduction

Flotation is a highly relevant separation process playing a major role in mineral processing, waste water treatment, or paper production. In mineral processing, it is used to separate the valuable minerals from the valueless gangue. To that end, the ore is crushed to small particles in the range of 20 to 200 µm.These particles are conditioned in the pulp by flotation reagents, mainly collector and frother molecules. Their function is to render the surface of valuable particles hydrophobic (collectors) while the frother supports the formation of a relatively stable froth later on the pulp.The conditioned pulp is introduced into large mechanical flotation cells, the size of which can range up to 600 m^3. At the bottom of the flotation cell, small gas bubbles are introduced by turbulent mixing. The valuable, hydrophobic particles attach to the bubble surfaces and are transported to the froth formed above the pulp in the cell. The froth contains both the valuable particles but also a small amount of entrained and undesired hydrophilic particles. By adding counter-flowing wash water, it is attempted to remove these entrained particles from the froth. The froth is permanently skimmed off from the flotation cell to extract the concentrate of valuable material in high grade [1].

Beside the particle-bubble attachment in the pulp, the effectiveness of the flotation process is highly dependent on the movement of hydrophilic and hydrophobic particles inside the froth. If the hydrophilic particles are not removed, the grade of the concentrate is low. On the other hand, if the wash water removes a part of the hydrophobic particles, the recovery rate is decreased. However, the behavior of the particles in the froth is not well investigated, because applicable measurement techniques scarcely exist [2].

Goodall et al. [3] use radioactively marked particles to track their movement in the froth by Geiger counters. Waters et al. [4,5] use radioactively marked, single particles inside a positron emission tomograph (PET) to track its movement from the pulp through the froth to the extract or back to the flotation cell. However, both techniques rely on tracking of single particles, which does not allow for measuring the instantaneous, three-dimensional distribution and movement of particles.

In a preliminary measurement campaign [6] we have demonstrated that neutron imaging (NI) is capable of determining both the liquid content of aqueous froth and of tracing single gadolinium particles inside the froth. This technique is now extended towards three-dimensional tracking of individual particles under realistic froth movement. Similar tracking in two dimensions has been carried out by Ščepanskis et al. [7] on particles in liquid metal flow using neutron imaging. However, in this work, a small pendulous rotation of the measurement object allows for three-dimensional reconstruction of particle tracks, motivated by tomosynthesis [8].

2 Method

2.1 Experimental Setup

The investigations are carried out inside a vertical cylindrical aluminum vessel of 67 mm diameter, 0.1 mm wall thickness and 130 mm height (see Fig. 1). The vessel is partially filled with deionized water, and a variable amount of sodium oleate (NaOl) and potassium chloride (KCl). At the bottom, bubbles are introduced by blowing 0.5 l/min pressurized air through a porous medium. By optical measurement, the initial bubble size is determined to equal 2 $\pm$ 0.5 mm. The bubbles rise and form a foam inside the vessel.

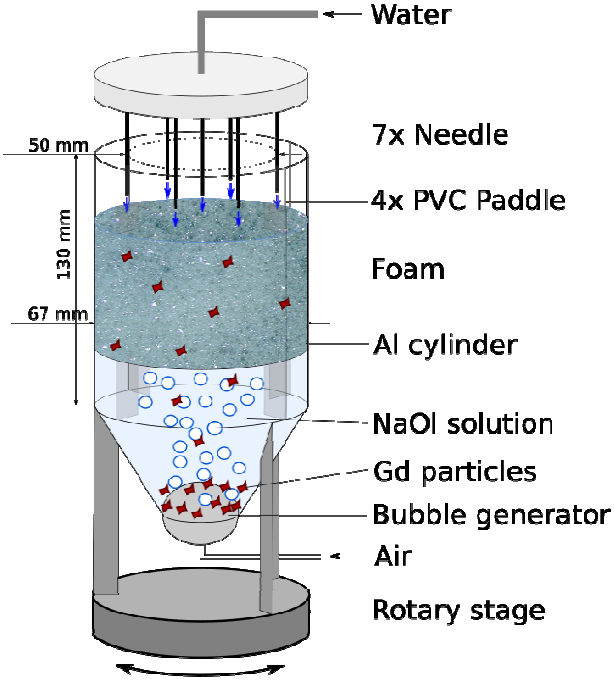

((Figure 1: Setup of the flotation experiment))

0.75 g Gadolinium (Gd) particles (sieved, d = 200-250 µm) are used as model particles due to their superior attenuation of neutrons. The particles were firstly hydrophobized by stirring them for 10 minutes in a solution of 2 mM NaOl and 10 mM KCl. Then, the particles were added to the vessel where they sunk to the bottom and rested on the bubble generator. When bubbles are generated, the Gd particles attach to the bubbles and enter the foam.

The whole vessel is mounted on a rotary stage. With a crank drive an oscillating angular motion

$$\Phi(t) = \Phi_0 \cdot \sin(\omega_0 \cdot t) \quad (1)$$

$$\dot{\Phi} = d\Phi/dt = \Phi_0 \cdot \omega_0 \cdot \cos(\omega_0 \cdot t) \quad (2)$$

withan amplitude $\Phi_0 = 10.3\,°$ and a frequency $\omega_0 = 2\pi \cdot 0.1\,Hz$ is applied. This rotary movement allows for the three-dimensional reconstruction. Inside the vessel four paddles are mounted that transfer the rotary movement onto the foam.

2.2 Neutron imaging

The Neutron imaging investigations were performed at the NEUTRA beamline, Swiss neutron spallation source SINQ, Paul Scherrer Institut. The collimated neutrons were transmitted through the measurement object that is placed in the vicinity of the detector. In the detector, the neutrons were captured by scintillator screen (^{6}LiF/ZnS 200µm) and the generated light and thus generated light was detected by sCMOS detector (HamamatsuORCA Flash 4.0). In that way, a radiographic image of the measurement object is recorded, as presented in Fig. (2). The time-series of radiographic images were taken continuously using 0.0667s

exposure time with 2 x 2 binning, thus leading to 1024 x 1024 pixels images with isotropic pixel size of 129 micrometers.

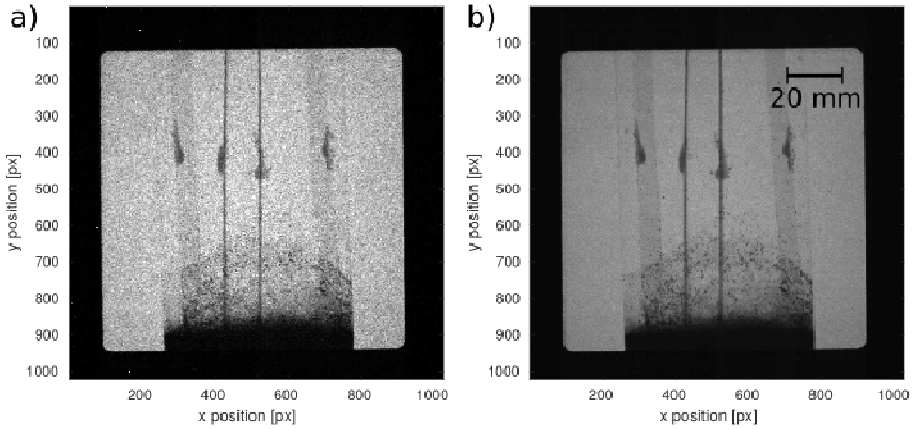

((Figure 2: Radiography images of the experiment, showing the vessel partially filled with foam containing 200 µm Gd particles. (a) Original image at 15 fps, (b) median-filtered image over 10 frames.))

The spatial resolution of this detection system used at these conditions has been limited to about 200 micrometres (i.e. to approximately 2 pixels).. A raw data example and the corresponding intensity profile of a cluster of particles in dry foam are shown in Fig. 3.

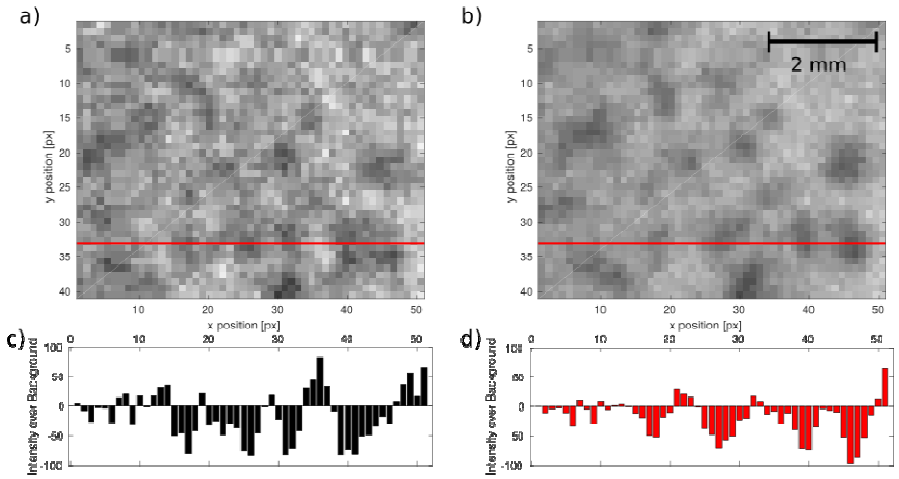

((Figure 3: (a,b) Radiographic image of a cluster of single Gd particles and (c,d) corresponding intensity distribution along the marked, horizontal line. (a,c) Original image at 15 fps, (b,d) median-filtered image over 10 frames.))

2.3 Image processing

In the post-processing, the three-dimensional tracks of particles are reconstructed by an algorithm consisting of three steps. In the first step, in each image all visible particles are detected. In the second step, these positions are assigned to tracks of individual particles. In the third step, the horizontal position of each particle along the beam direction is reconstructed.

Step 1: The recognition of particles in the images is problematic because the fast movement of the particles requires high frame rates and low exposure times. The low exposure time results in low intensity and a high noise level in the images. Additionally, the noise is not purely stochastic but shows coherent structures in the size of 3 pixel (see Figure 4a), which is close to the diameter of the particles.

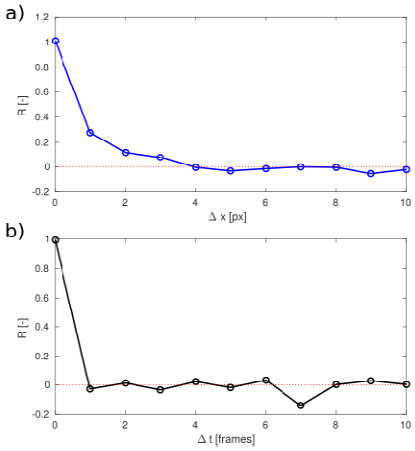

((Figure 4: Autocorrelation of the intensity distribution measured in the background region (a) over a vertical line of 500 px length in a single frame and (b) on a fixed pixel over 500 frames at 15 fps.))

This makes it very difficult to differentiate the particles from the noise. This issue has been solved by applying high frame rates and a sliding average over time (see Fig. 3), because the coherence time of the noise structure is well below the smallest reasonable exposure time. Subsequently, a template is generated, representing the expected image of a typical, single gadolinium particle, assuming spherical particles of equal diameter. Each position of the image is correlated with the template. Regions in the image that appear similar to the template yield high correlation coefficients (see Fig. 5). However, also regions with high gradients in brightness show high correlation coefficients, which will be filtered later.

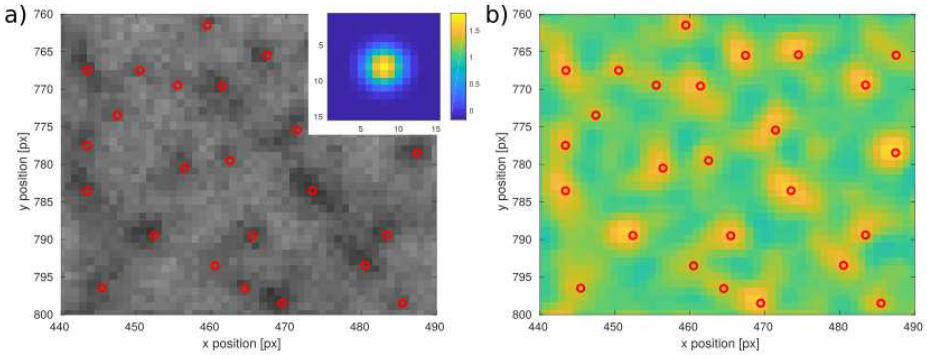

((Figure 5: (a) Mean-filtered radiography of a cluster of particle. The inset shows the applied template for particle detection. Correlating the radiography with the template results in the correlation distribution shown in b) where a peak-finder detects particles (red circles in both images).))

Using the MATLAB particle tracking program provided by Blair and Dufresne [9] peaks are detected in the correlation distribution, corresponding to candidates for particles.

Step 2: Constructing the particle tracks has also been carried out with the MATLAB particle tracking program provided by Blair and Dufresne [9]. The acceptable gap in time that a particle may disappear along the track is set to one frame. A total signal length of at least 15 frames is required to classify a track as an actual particle track. In that way, falsely detected peaks are removed. In each frame approximately 50 % of the candidates from Step 1 are removed by this criterion.

Step 3: From the reconstructed path x(t),y(t) in the image now the three-dimensional track inside the cylinders reference system h(t), r(t), φ(t) is reconstructed (see Fig. 6).

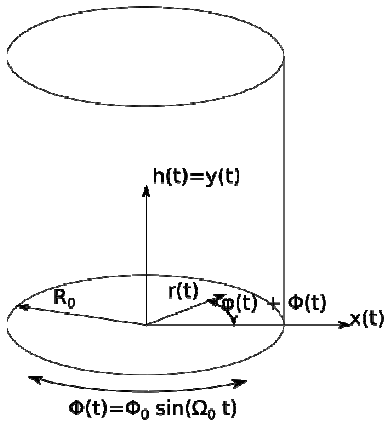

((Figure 6: Relation between the (x,y) coordinate system of the camera and (h, r, φ)reference system in the rotating cylinder.))

The height h(t) directly coincides with the vertical position y(t) = h(t). The horizontal position x(t) corresponds to

$$x(t) = r(t) \cdot \cos(\varphi(t) + \Phi(t)) \qquad (3)$$

Assuming, that the horizontal movement inside the cylinders frame of reference is negligible, the horizontal velocity results only from the rotation of the flotation cell, yielding

$$dx(t)/dt = -r(t) \cdot \sin(\varphi(t) + \Phi(t)) \cdot \dot{\Phi}(t) \qquad (4)$$

The horizontal velocity of each particle is computed along its track by linear fitting its horizontal movement $x = a \cdot t + b$along 15 frames, yielding a discretization error typically below five percent. The corresponding horizontal position x(t) is taken from the central frame, i.e. frame number 8. Subsequently the angular position φ(t) is derived from the ratio between horizontal velocity and position given by

$$\varphi(t) = \arctan\left[(dx(t)/dt)/\left(x(t) \cdot \dot{\Phi}(t)\right)\right] - \Phi(t) + \pi/2 \cdot (1 - sgn(x)) \qquad (5)$$

Subsequently, r(t) is derived from Eq. (3). This approach is only exact, if the horizontal velocity of the particles inside the cylinders frame of reference equals zero. The linear fit provides a very effective and reasonable smoothing of the paths, leading to plausible results. After the reconstruction, particle tracks with a detected position outside the flotation cell have been removed. But, this has been necessary only for a very limited number of particle tracks. A typical cloud of reconstructed particle tracks is shown in Fig. 7.

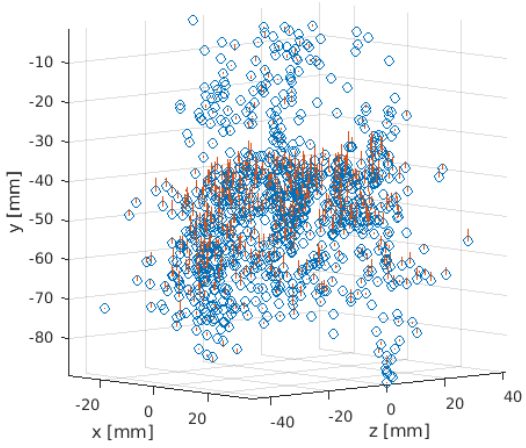

((Figure 7 Tracking results for high frother concentration showing three-dimensional particle position and vertical velocity.))

3 Results

Three different concentrations (a: 50 µM, b: 32 µM, c: 20 µM) of the frother NaOl have been employed. The other parameters have been kept constant.

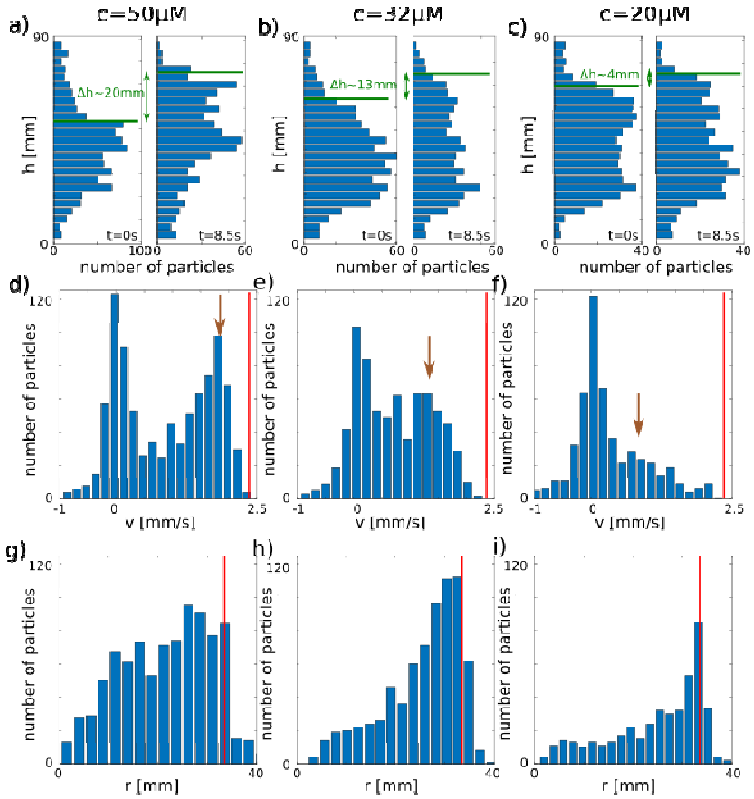

((Figure 8 Tracking results for three different frother concentrations in three columns. (a,b,c) height distribution in two points in time with 8.5 seconds difference. (d,e,f) vertical velocity of all tracked particles for the first time instance. The vertical red line marks the superficial gas velocity. (g,h,i) radial distribution of all tracked particles. The vertical line marks the container radius.))

Figures 8a-c show the number of tracked particles over height at two points in time separated by a Δt=8.5 sec. The green line visualizes the approximate vertical position of the surface of the froth. Derived from the gas flow rate it should move with 20.5 mm per 8.5 sec. This is in good agreement with figure 8a, where the highest frother concentration is used. With decreased concentration bubble rupture takes place and the superficial froth velocity is decreased and in figure 8c nearly a steady froth height is reached.
Figures 8d-f show the vertical velocity of all tracked particles. The red line marks the velocity corresponding to the superficial gas velocity. The particle velocities show a bimodal distribution, consisting of particles sticking on the wall and mobile particles. The particles at the wall have a vertical velocity close to zero. The mobile particles move upwards with a velocity below the superficial gas velocity. The upward velocity of the mobile particles (marked by an arrow in the figures 8d-f) decreases with decreasing frother concentration, because film rupture leads to agglomeration of particles which experience higher gravity forces and are less well carried by the gas flow. With decreasing frother concentration also the ratio of mobile particles decreases. This is supported by the figures 8g-i, demonstrating an increasing amount of particles close to the radial position of the cylinder wall. This is due to the fact, that bubble rupture events enhance horizontal transport of the particles and due to their hydrophobicity the particles stick at the wall once they touch it.

4 Discussion

In this work, neutron imaging has revealed the movement of gadolinium particles inside froth. The technique allows to track individual particles of size of 200 µm and larger with the position resolution of one pixel,

corresponding to 129 micrometers. Smaller particles could not be identified individually. However, they might accumulate in vertices of the foam structure [5] forming trackable clusters. At the same time, the number of particles and the total gadolinium amount in such clusters cannot be measured. Although the quantitative measurement of mass flux in the froth may contain a certain uncertainty, the big advantage of the technique is the ability to identify flux routes of particles and liquid content.

There are certain limitations in the present technique. Sudden particle motions of high velocity, as arising from lamella rupture events, which were observed at low frother concentrations, are not detectable at the moment. However, with higher neutron flux at a different beamline or in an upgraded version of the spallation source higher frame rates are achievable allowing for tracking of faster movement.

The present reconstruction algorithm is less exact for positions of $\varphi(t) + \Phi(t) = k\,\pi$, because the visible horizontal velocity $dx(t)/dt$ vanishes ans thus, the result of the arctan-term in Equation (5) is less sensitive. Consequently, the angular position can be derived only with a high uncertainty in these regions. However, the radial position $r(t)$ is less sensitive on the angular position in Equation (3), when $\varphi(t) + \Phi(t) = k\,\pi$. Consequently, the uncertainty of the radial position is not increased in these regions.

Higher rotary speed of the cylinder would improve the 3D reconstruction of the particle tracks. This would also increase inertia and centrifugal forces on the particles, biasing the particle movement. In the present experiment, inertia forces on the particles are below 0.1% of gravity and centrifugal forces below 0.01%, which is sufficiently small. The reason for the low rotary speed in the present experiment was the limited frame rate due to high noise. With higher neutron flux, this could easily be increased.

In general, particle tracking in froth allows for determining the trajectories of gadolinium particles inside the froth and thus, investigate the recovery process and drop-back event in dependence on wash-water addition as well as frother and collector concentrations. Even though the field of view is limited to 10x10 cm^2, this technique could provide valuable information on the froth in a flotation cell.

Acknowledgments

Financial support of the German research foundation (HE/8571-1) is gratefully acknowledged. This work is based on experiments performed at the Swiss spallation neutron source SINQ, Paul Scherrer Institut, Villigen, Switzerland.

Literature

[1] Fuerstenau, Maurice C., Graeme J. Jameson, and Roe-Hoan Yoon, eds. *Froth flotation: a century of innovation*. SME, 2007.
[2] Meng, J., Tabosa, E., Xie, W., Runge, K., Bradshaw, D., &Manlapig, E. (2016). A review of turbulence measurement techniques for flotation.*Minerals Engineering*, *95*, 79-95.
[3] Goodall, C. M., and C. T. O'Connor. "Pulp-froth interactions in a laboratory column flotation cell."*Minerals Engineering* 4.7-11 (1991): 951-958.
[4] Waters, K. E., Rowson, N. A., Fan, X., Parker, D. J., &Cilliers, J. J. (2008). Positron emission particle tracking as a method to map the movement of particles in the pulp and froth phases.*Minerals Engineering*, *21*(12-14), 877-882.
[5] Cole, K., Brito-Parada, P. R., Morrison, A., Govender, I., Buffler, A., Hadler, K., &Cilliers, J. J. (2015). Using positron emission tomography (PET) to determine liquid content in overflowing foam.*Chemical Engineering Research and Design*, *94*, 721-725.
[6] Heitkam, S., Rudolph, M., Lappan, T., Sarma, M., Eckert, S., Trtik, P., Lehmann, E., Vontobel, P., & Eckert, K. (2018). Neutron imaging of froth structure and particle motion. *Minerals Engineering*, 119, 126-129.
[7] Ščepanskis, M., Sarma, M., Vontobel, P., Trtik, P., Thomsen, K., Jakovičs, A., & Beinerts, T. (2017). Assessment of electromagnetic stirrer agitated liquid metal flows by dynamic neutron radiography. *Metallurgical and materials transactions B*, 48(2), 1045-1054.
[8] Levakhina, Y. (2014). *Three-Dimensional Digital Tomosynthesis: Iterative reconstruction, artifact reduction and alternative acquisition geometry*. Springer.

[9] D. L. Blair and E. R. Dufresne, The Matlab Particle Tracking Code Repository,
http://physics.georgetown.edu/matlab/.